Analog Dialogue

Volume 42, Number 3, 2008 | A forum for the exchange of circuits, systems, and software for real-world signal processing

In This Issue

Analog Dialogue Since 1967

www.analog.com/analogdialogue

ANALOG DEVICES

Editors' Notes

FINGERPRINTS, BLOOD, AND DEFECTIVE RAILS

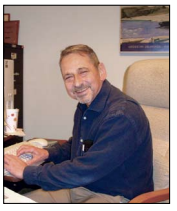

Whether you access a computer, enter a secure building, or go on a trip, biometric sensors simplify effective identification. *Fingerprinting* has a long history of unique identification for individuals; modern scanning equipment eliminates inky fingers and delays in verifying ID. See the article on Page 3 for insights into sensors, feature extraction, pattern matching, and decision making in fingerprint-based equipment.

Blood forms clots to end bleeding at an injured site—a good thing, unless the site is involved in a surgery where blood must keep flowing, as in a heart-lung machine during heart-bypass surgery. In such instances, an anticoagulant is administered during surgery; but the process must be rapidly reversed at the end of the surgery. In controlling the process, it is important to know when coagulation is actually occurring. Coagulation monitoring, see Page 7, uses impedance measurement to provide rapid, automated data—aiding patient safety, workflow, and decision making—and leads to improved outcomes.

Effective, efficient, reliable rail transportation with comfort and safety depends on the soundness of fixed infrastructure, such as rails and roadbeds. This is especially relevant in urban public transportation, with its stresses of rapid acceleration and deceleration. Starting on Page 10, we describe how a new systematic maintenance approach—now going into use in Europe—makes it possible to measure, locate, and fix rail- and tramway defects early on. Key to its effectiveness are mature railway-engineering know how and cutting-edge automated technologies, including Blackfin processors, satellite-based location, detailed record-keeping, and graphical system design techniques.

FOURSCORE

As the 3rd quarter of 2008 ends, we (Dan) have completed another year—our 80th—of breathing Earth's air, of processing food, beverages, images, sounds, smells, tastes, shapes, temperatures, feelings—and *ideas*. Coincidentally, as the first quarter of 2009 begins, a two-score stretch (half) of those years, will have been in the service of Analog Devices and the readers of this Journal—and perhaps even their children and/or parents.

We came to ADI after nearly a score of years at George A. Philbrick Researches, Inc. There, originally immersed in *analog computing* technology and applications, our later publications and products established a market for plug-in *operational amplifiers* as versatile precision circuit components—a market that in time grew to be dominated by Analog Devices.

Our mission, on joining ADI in 1969—besides the *Dialogue*, then in its 3rd year (now nearing 42 years in print and 10 online), was to assemble a book that would educate a world of unsuspecting (and some yet unborn) engineers about the nature, applications, pitfalls, and minutiae of *analog-to-digital* and *digital-to-analog converters*. The *Analog-Digital Conversion Handbook*, published in 1972, coincided with a line of converters based on Jim Pastoriza's precision IC quad current source. That combination sparked a market in which ADI's data-converter leadership and dominance has grown continuously over the years.

Soon Barrie Gilbert joined us—and Lew Counts—in advocating long-simmering ideas from early Philbrick days about market possibilities for instrumentation circuits with analog computing elements: *multiplying*, *logarithmic*, and *rms* devices. Subsequent publication of the *Nonlinear Circuits Handbook* led to ADI's primacy in this somewhat recondite area of analog technology.

Exploiting a fundamental semiconductor property, *proportional to absolute temperature* (PTAT), led to the introduction of precision temperature-measuring ICs (and their corollary: temperature-insensitive voltage references) and inspired publication of the *Transducer Interfacing Handbook*.

The watershed books mentioned above are out of print (but perhaps yet available via *Amazon.com*). ADI's applications engineers continue to produce timely books in support of our technologies. You can find them at analog.com/analogdialogue; click on "Potpourri," and then on "Books." And watch for possibly new books to promote seminal technologies that, as in the past, introduce unanticipated useful tools.

Dan Sheingold [dan.sheingold@analog.com]

ANALOG ICs POWER DIGITAL TVs

At midnight on February 17, 2009, most commercial analog TV broadcasts—long the U.S. standard—will cease, leaving the more flexible and efficient digital television (DTV) broadcasts to rule the video airwaves. Bandwidth will be freed for new telecommunications applications, including ultrafast wireless broadband, mobile TV, and public safety/emergency communication systems.

Don't confuse *digital television* with *high-definition television* (HDTV). DTV refers to the transmission technology, which can carry high definition, standard definition, or data; whereas, HDTV refers to broadcasts of high-resolution pictures. Digital technology and error correction techniques enable reception of crystal-clear pictures and sound, without ghosts, snow, or other artifacts, if the signal level is adequate; otherwise, the error frequency will increase beyond the correction threshold, and the picture will be lost entirely—an all-or-nothing proposition.

Broadcasts from DTV stations using *multicasting* can replace a single analog channel by up to four channels of programming. They can deliver data services that analog technology can't provide, including program information and the latest news, weather, sports scores, and traffic updates. Future interactive video services will enable viewers to play additional media elements embedded in the main program.

How will this transition affect you? 85% of all TV viewers—subscribers to cable, satellite, or other pay services—will be essentially unaffected. But free over-the-air broadcasts will no longer be available to those with older analog TVs using standard antennas. Three basic choices are available: connect to cable, satellite, or other pay service (with its set-top box); purchase a new digital TV receiver; or add a converter box to the existing analog TV system (the latter's $40 to $60 cost may be partially subsidized by $40 coupons from the U.S. government).

Many see the digital television transition as burdensome, but for some, free DTV can replace expensive pay TV. If viewers are satisfied by the broadcast programming from ABC, CBS,

(continued on Page 15)

Analog Dialogue

www.analog.com/analogdialogue **dialogue.editor@analog.com**

Analog Dialogue is the free technical magazine of Analog Devices, Inc., published continuously for 42 years—starting in 1967. It discusses products, applications, technology, and techniques for analog, digital, and mixed-signal processing. It is currently published in two editions—*online*, monthly at the above URL, and quarterly *in print*, as periodic retrospective collections of articles that have appeared online. In addition to technical articles, the online edition has timely announcements, linking to data sheets of newly released and pre-release products, and "Potpourri"—a universe of links to important and rapidly proliferating sources of relevant information and activity on the Analog Devices website and elsewhere. The *Analog Dialogue* site is, in effect, a "high-pass-filtered" point of entry to the **www.analog.com** site—the virtual world of *Analog Devices*. For history buffs, the *Analog Dialogue* archives include all regular editions, starting with Volume 1, Number 1 (1967), plus three special anniversary issues.

If you wish to subscribe to the print edition, please go to **www.analog.com/analogdialogue** and click on **<subscribe>**. Your comments are always welcome; please send messages to **dialogue.editor@analog.com** or to these individuals: *Dan Sheingold*, Editor **[dan.sheingold@analog.com]** or *Scott Wayne*, Managing Editor and Publisher **[scott.wayne@analog.com].**

ISSN 0161-3626 ©Analog Devices, Inc. 2008

Fingerprint Sensor and Blackfin Processor Enhance Biometric-Identification Equipment Design

By Jayanti Addepalli and Aseem Vasudev

Biometrics and Security

The need for effective security, implemented efficiently, is manifest in today's world. Individuals must be identified to allow or prohibit access to secure areas—or to enable them to use a computer, personal digital assistant (PDA), or mobile phone. Biometric signatures, or *biometrics*, are used to identify individuals by measuring certain unique physical and behavioral characteristics. Virtually all biometric techniques are implemented using a *sensor*, to acquire raw biometric data from an individual; *feature extraction*, to process the acquired data to develop a feature-set that represents the biometric trait; *pattern matching*, to compare the extracted feature-set against stored templates residing in a database; and *decision-making*, whereby a user's claimed identity is authenticated or rejected.

Fingerprint Sensors

Fingerprints, long one of the most widely accepted biometric identifiers, are unique and permanent. Their images, formed of multiple curve segments, comprise high areas called *ridges* and low areas called *valleys*. *Minutiae*, the local discontinuities in the ridge flow pattern, are used as discriminating features. Fingerprint sensors "read" the finger surface and convert the analog reading into digital form through an analog-to-digital converter (ADC). Fingerprint sensors can be broadly classified as optical, ultrasound, or solid state—which includes capacitive, RF, thermal, and piezoelectric devices.

Because a finger's outermost dry, dead skin cells have low electrical conductivity, an *RF sensor* acquires fingerprint data from the skin's moist and electrically conductive boundary region where the live cells begin turning into keratinized skin. This live subsurface layer is the source of the fingerprint pattern, and it is rarely affected by damage or wear to the finger surface.

The AuthenTec®[1] TruePrint®[2] sensor uses a small RF signal between a conductive layer buried inside the silicon chip and the electrically conductive layer just below the surface of the skin. The RF field measures the electrical potential contours of the ridges and valleys of the finger's underlying live epidermal layers. By acquiring data from the part of the skin that is untainted by injury or contamination, the sensor produces a more accurate and repeatable fingerprint sample than alternative optical or capacitive technologies that read only the surface of the skin.

Pyroelectric materials generate a voltage based on temperature differentials. When a finger is in contact with a warmed sensor's surface, the fingerprint ridges—which are closer to the sensor surface—retain a higher temperature than the valleys, which are farther from the sensor surface. The Atmel® AT77C104B[3] FingerChip® sensor captures fingerprints using this type of thermal imaging. A linear sensor, it combines detection and data conversion circuitry in a single CMOS IC. Fingerprint images are captured by sweeping the finger over a sensing area. An image is produced when contact first occurs, but because it soon disappears as thermal equilibrium is reached, a sweeping method is necessary to acquire a stable fingerprint image.

The sensor, shown in Figure 1, captures the image of a fingerprint as the finger is swept vertically over the sensor window, as shown in Figure 2. The finger sweep technology ensures that the sensor surface stays clean. Unlike touch-based sensors, latent fingerprints do not remain once the finger has been removed. The sensor requires no external heat, light, or radio source. On-chip temperature stabilization identifies a temperature difference between the finger and the sensor, and increases the difference for higher image contrast. The discussion here will focus on a fingerprint recognition system based on this type of thermal sensor.

Figure 1. AT77C104B FingerChip IC.

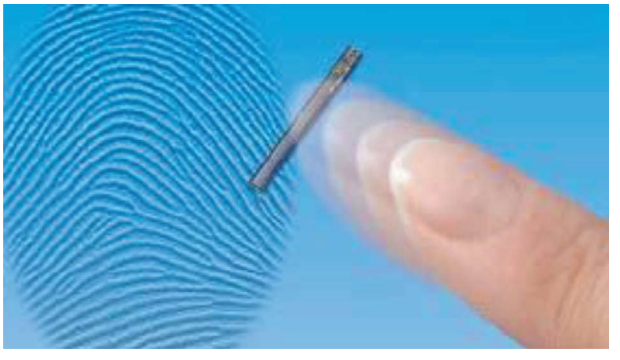

Figure 2. Typical fingerprint—and finger being swept over a sensor.

The main parameters that characterize fingerprint sensors include *resolution*, *area*, *dynamic range*, and *number of pixels*. *Resolution* is measured in dots (or pixels) per inch (dpi). Higher resolution allows better definition between ridges and valleys, and finer isolation of minutiae points—which play a primary role in fingerprint matching, since most algorithms rely on the coincidence of minutiae to determine if two fingerprint impressions are of the same finger. Larger sensing *areas* generally provide a more distinctive fingerprint, but sweeping the finger over a smaller sensor, and acquiring and processing the data rapidly, allows a small, low-cost sensor to achieve comparable definition to larger, more expensive sensors. *Dynamic range*, or depth, denotes the number of bits used to encode the intensity of each pixel. The *number of pixels* in the fingerprint image in a particular frame can be derived from the resolution and area.

The AT77C104B sensor has 500-dpi resolution over a 0.4 mm × 11.6 mm area, providing a total of 8 pixels × 232 pixels, or 1856 pixels per frame. Each pixel is encoded with four bits,

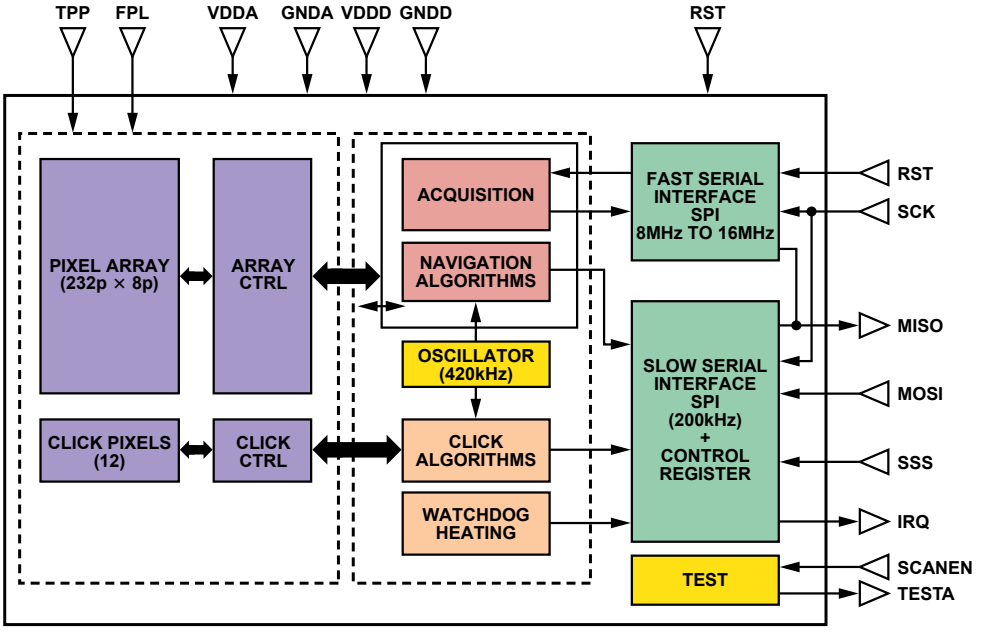

Figure 3. Block diagram of the fingerprint sensor.

identifying 16 grayscale levels. Figure 3 shows a block diagram of the sensor, which includes the array, analog-to-digital converter, on-chip oscillator, control and status registers, navigation and click units, and separate interfaces for *slow* and *fast* modes of operation. Slow mode, which can run at up to 200 kHz, is used to program, control, and configure the sensor. Fast mode, which can run at up to 16 MHz, is used for data acquisition. An on-chip heater increases the temperature difference between the finger and the sensor. To limit current consumption, a watchdog timer stops heating the module after a specified length of time.

Modes of Operation

The sensor implements six modes of operation:

- *Sleep* mode: A very low-power-consumption mode, in which the internal clocks are disabled and the registers are initialized.
- *Standby* mode: A low-power-consumption mode, waiting for action from the host. The slow serial port interface (SSPI) and control blocks are activated; the oscillator remains active.
- *Click* mode: Waiting for a finger on the sensor. The SSPI and control blocks remain active; the local oscillator, click array, and click block are activated.
- *Navigation* mode: Calculating *x*- and *y* movements as the finger crosses the sensor. The SSPI and control blocks are still activated; the local oscillator, navigation array, and navigation block are also activated.
- *Acquisition* mode: Slices are sent to the host for fingerprint reconstruction and identification. The SSPI and control blocks are still activated; the fast serial port interface block (FSPI) and the acquisition array are activated. The local oscillator is activated when a watchdog timer is required.
- *Test* mode: This mode is reserved for factory testing.

Interfacing the Fingerprint Sensor to the Blackfin® Processor's Serial Peripheral Interface

The Blackfin ADSP-BF533[4] low-cost, high-performance processor is chosen for this application because it combines the functions of a fast signal processor and a powerful microcontroller. Its 4-wire, full-duplex synchronous serial peripheral interface (SPI) has two data pins (MOSI and MISO), a device-select pin ($\overline{\text{SPISS}}$), and a gated clock pin (SCK). See Figure 4. The SPI supports *master* modes, *slave* modes, and *multimaster* environments. The SPI-compatible peripheral implementation also supports programmable baud rate and clock phase/polarities.

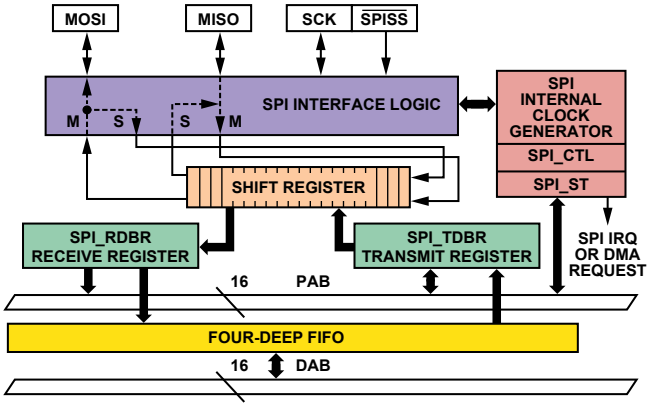

Figure 4. Block diagram of Blackfin processor's SPI port.

The interface is essentially a shift register that serially transmits and receives data bits—one bit at a time, at the SCK rate—to and from other SPI devices. The shift register enables the simultaneous transmission and reception of serial data. The SCK synchronizes the shifting and sampling of the data on the two serial data pins.

The SPI port can be configured as *master* (generates SCK and $\overline{\text{SPISS}}$ signals) or *slave* (receives SCK and slave select signals externally). When the SPI port is configured as master, it drives data on the MOSI pin and receives data on the MISO pin. It drives the slave select signals for SPI slave devices and provides the serial bit clock (SCK). The Blackfin processor's SPI supports four functional modes by using combinations provided by the clock polarity (CPOL) and clock phase (CPHA) bits. For detailed information on the Blackfin SPI port, refer to the ADSP-BF533 Blackfin Processor Hardware Reference Manual.[5]

Hardware Interface

The seamless hardware interface between the ADSP-BF533 processor's SPI port and the AT77C104B, shown in Figure 5, does not require any external glue logic. The *slave select* signals of the sensor, $\overline{SSS}$ and $\overline{FSS}$, are driven through programmable flag pins PF1 and PF2. One flag should be configured as an output and driven high before the other flag is configured as an output (these flags should never be simultaneously configured as outputs, as the Blackfin processor, driving them low by default, would switch the sensor chip to scan test mode). Sensor interrupts, generated through the $\overline{IRQ}$ pin, are read by input PF4. The reset, RST, is driven by PF3. Reset is an active-high signal, so a pull-down resistor is used on this line.

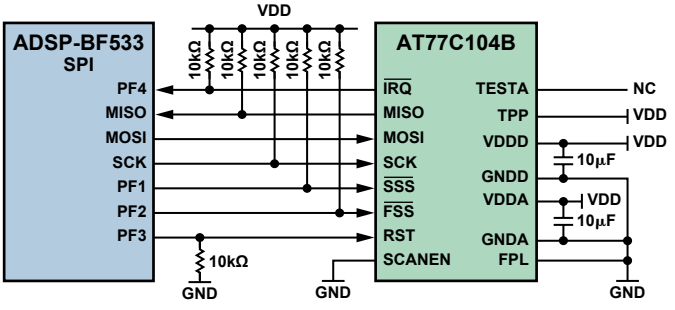

Figure 5. Interface between ADSP-BF533 processor and AT77104B FingerChip sensor.

Application Software

The application code performs tasks such as controlling the sensor, acquiring fingerprint data, and rearranging the data to display the received fingerprint image using the VisualDSP++®[6] development tool's Image Viewer plug-in.

When the sensor detects a *click* (i.e., a signal indicating the presence of a finger), it generates an interrupt. The Blackfin processor receives this interrupt, and generates an interrupt on a falling edge. The STATUS register indicates the event that caused the interrupt. This process is used for navigation, read error, and other interrupts. A simplified flow chart of the complete application is shown in Figure 6.

Data Acquisition

Sensor heating is enabled in acquisition mode. The watchdog timer is also enabled, ensuring that heating remains controlled. Thus, when heating is requested, the sensor is heated for *n* seconds.

DMA parameters are then set up for data acquisition. Variable-size DMA flex descriptors are loaded into DMA parameter registers. The sequence of registers is essentially fixed, but the length of the descriptor is completely programmable. A 2D array is used to configure the DMA parameters. The 1D arrays are the individual descriptors. The first descriptor, a dummy, is used to receive the first five bytes because 40 dummy clock cycles must be sent by the sensor before the first data arrives in order to initialize the chip pipeline. Thus, the first synchronization sequences appear after 40 clock cycles. Data then arrives at every clock cycle for all following array readings.

The sensor sends data in the form of *frames*. The start of each frame is marked by the dummy column, which contains a synchronization word. The pixel array is read top to bottom, column by column, from the top left to the bottom right.

Data Rearrangement

The data must be rearranged to display the acquired fingerprint image. The rearranged data is stored and can be viewed using the VisualDSP++ ImageViewer utility. The acquired image and settings are shown in Figure 7. The following functions are performed:

- *Nibble-swapping*: The sensor sends data in a nibble-swapped format. A routine swaps the odd-even pixels for the entire frame.
- *4-bit to 8-bit conversion*: Each sensor pixel is 4 bits wide, but the Image Viewer displays images with 8-pixel minimum width. Four bits of zero-padding converts each pixel to 8 bits.
- *Level adjustment*: Each pixel in the received data has an intensity of 0 to 15, but the display range is 0 to 255. Level translation of each pixel produces a good display.
- *Array transpose*: The data from the sensor is sent column-wise, but the 2-dimensional DMA receives data row-wise, so it must be transposed in order to display the frames continuously. A 3-dimensional array is used to get a continuous display of frames.

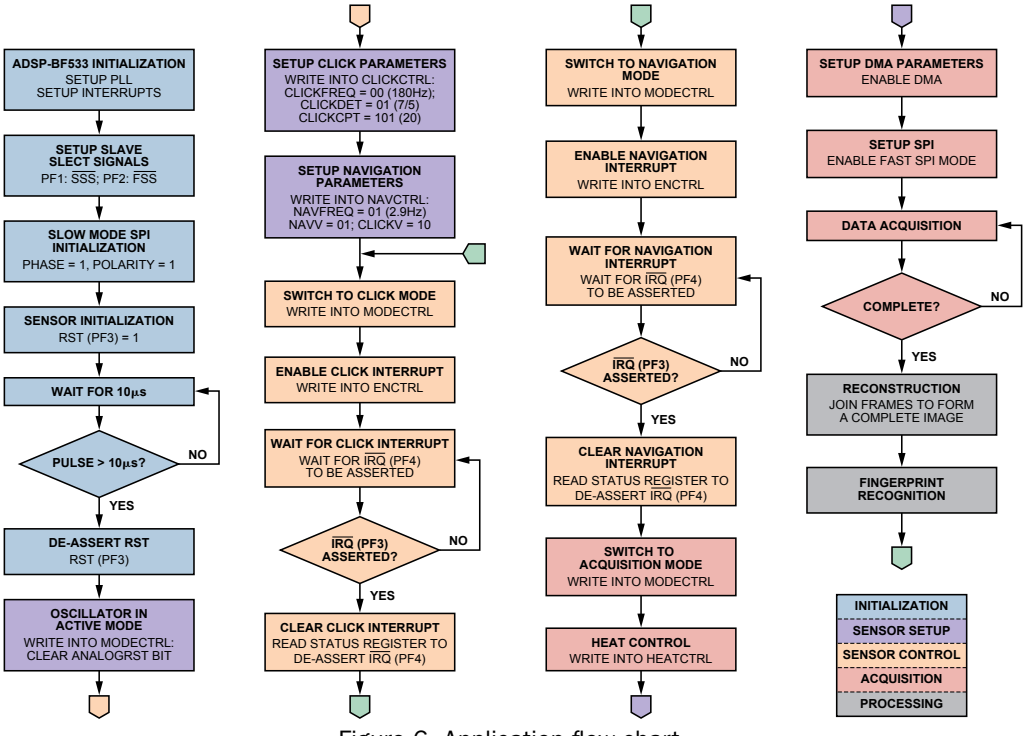

Figure 6. Application flow chart.

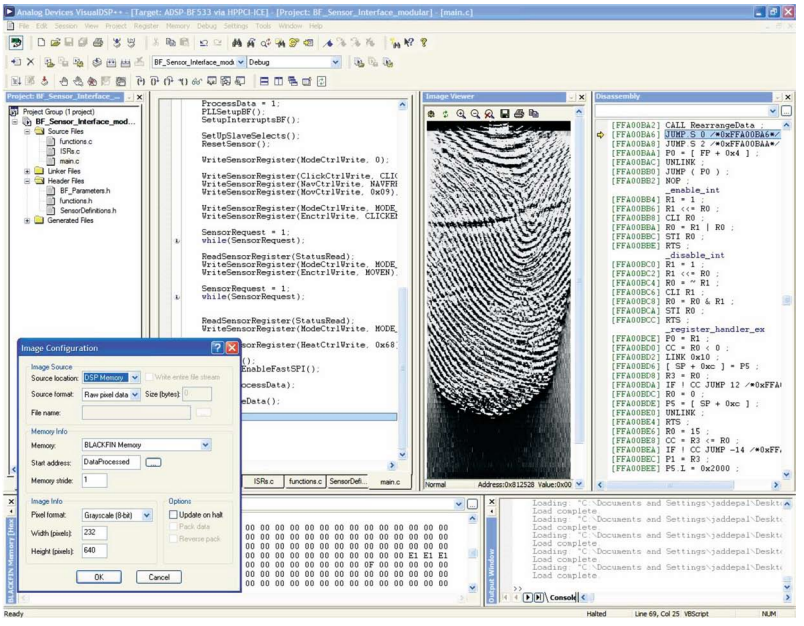

Figure 7. VisualDSP++ screen shot for image capture.

Fingerprint Reconstruction and Recognition

If the fingertip is swept across the sensor window at a reasonable rate, the overlap between successive frames enables an image of the entire fingerprint to be reconstructed using software supplied by Atmel. The reconstructed image is typically 25 mm × 14 mm, or 500 pixels × 280 pixels, with 8-bit resolution due to resolution enhancement. Each image thus requires 140 kB of storage. Larger or smaller images can be derived from this using standard image-processing techniques. Once the frames have been joined to obtain a complete fingerprint image, recognition algorithms can match the sample with a template.

Trust but Verify

Fingerprint processing has three primary functions: *enroll*, *search*, and *verify*. *Enrollment* acquires a fingerprint image from the sensor and saves it in SRAM. The image is processed, enhanced, and compressed to create a fingerprint template. Various filters clean up the image and convert it to a mathematical representation, making it impossible to steal a template and directly recreate a fingerprint image.

Search compares a raw candidate image to a list of previously enrolled templates. Through a series of screening processes, the algorithm narrows the list of templates to a manageable size. Those templates that survive screening are compared to the candidate and verification scores are provided. A score exceeding a preset threshold indicates a positive identification.

Verification validates a user's identity by comparing a raw candidate image to a previously enrolled template via real-time, closed-loop pattern-matching algorithms. A score is returned indicating the similarity of the candidate and template to generate a yes/no match decision.

CONCLUSION

The Blackfin processor and AT77C104B FingerChip sensor combine to provide simple, yet robust, fingerprint identification, enhancing security by allowing or prohibiting access to sensitive areas in buildings or sensitive data in laptop computers.

FURTHER READING

1. ADI website: www.analog.com (Search) Blackfin Processors (Go)
2. ADI website: www.analog.com (Search) VisualDSP++ (Go)
3. *ADSP-BF53x/ADSP-BF56x Blackfin Processor Hardware Programming Reference*. Analog Devices. 2007.
4. ADSP-BF531/ ADSP-BF532/ADSP-BF533 Blackfin Embedded Processor Data Sheet.
5. AT77C104B Data Sheet. "FingerChip Thermal Fingerprint Sweep Sensor." Atmel Corporation.
6. "AuthenTec Speeds Fingerprint Matching with Blackfin." *Blackfin Customer Case Studies*. Dec 2004.
7. Interfacing Atmel Fingerprint Sensor AT77C104B with Blackfin Processors. Engineer to Engineer Note EE-325. Aug 2007.
8. Kreitzer, Kelvin and Alan Kasten. "New Fingerprint Subsystem Brings Biometrics to the Mass Market." *Embedded Computing Design*. 2007.
9. Maltoni, David, Dario Maio, Anil K. Jain, and Salil Prabhakar. *Handbook of Fingerprint Recognition*. Jun 2003.

REFERENCES

[1] www.authentec.com.

[2] www.zvetcobiometrics.com/Documents/Trueprinttechnology.ppt#303,1. TruePrint Technology The Fundamentals.

[3] www.atmel.com/dyn/resources/prod_documents/doc5347.pdf.

[4] ADI website: www.analog.com (Search) ADSP-BF533 (Go)

[5] www.analog.com/static/imported-files/processor_manuals/892485982bf533_hwr.pdf.

[6] www.analog.com/en/embedded-processing-dsp/blackfin/VDSP-BF-SH-TS/products/product.html.

THE AUTHORS

Jayanti Addepalli [jayanti.addepalli@analog.com] is a DSP applications engineer with the India Product Development Center (IPDC) Applications Group in Bangalore, India. She joined Analog Devices in June 2006 after graduating from National Institute of Technology, Warangal, with a BTech in electronics and communications engineering. She works primarily on application development involving Blackfin processors.

Aseem Vasudev [aseem.v@analog.com] joined ADI in 2002 as a processor applications engineer, located in Bangalore, India. Previously he worked as a senior system design and VLSI engineer at Tata Infotech, Wipro Technologies, and Force Computers. He received a BE in electrical and electronics engineering in 1997.

Impedance Measurement Monitors Blood Coagulation

By Helen Berney and J.J. O'Riordan

INTRODUCTION

Blood coagulation is a complex, dynamic physiological process by which clots are formed to end bleeding at an injured site. During heart-bypass surgery, blood is diverted out of the body to a heart-lung machine, which maintains heart- and lung functions. The machine is operated by a *perfusionist*, whose role includes monitoring appropriate parameters to ensure that the patient is effectively treated with an anticoagulant to avoid blood clots. For this purpose, heparin, an anticoagulant drug, is administered during surgery—followed by a rapid reversal afterwards to prevent excessive bleeding.[1] To maintain the delicate balance between clotting and bleeding, the clotting time of the patient is monitored every 30 to 60 minutes during surgery and several times after surgery, until a normal clotting time is restored.[2] Currently, blood samples taken from a patient's intravenous line are tested at bedside, with measured clotting-time values used to adjust the anticoagulation therapy.

Analog Devices is a partner in the Biomedical Diagnostics Institute (BDI),[3] a Centre for Science, Engineering, and Technology, funded by Science Foundation Ireland.[4] BDI is a multidisciplinary research institute focused on the development of next-generation biomedical diagnostic devices. Under one of the BDI Integration Programs, Analog Devices is working with Dublin City University[5] and a global specialty pharmaceutical and medication delivery company to develop a coagulation-monitoring device for patients undergoing treatment in the critical-care environment. This system will provide rapid, automated information on patient clotting status—improving patient safety, workflow, and decision support—leading to improvements in patient outcomes.

Electrical Measurement of Blood Coagulation

Blood coagulation in the body is modulated by a number of cellular and other active components. The *coagulation cascade* describes the components of blood and how they are involved in the process of clot formation. As the cascade becomes activated, the blood progresses from a nonclotting to a clotting state, causing changes in both molecular charge states and effective charge mobility. The final steps of the cascade involve two components, *thrombin* and *fibrinogen*. Thrombin acts by cutting the fibrinogen, forming fibrin filaments—which spontaneously aggregate. The endpoint of clotting time has been defined as the time at which a fibrin clot is formed.[6,7]

By monitoring the global impedance of a clotting blood sample, the changes in conductivity associated with clot formation are measured. To evaluate instrument performance, the clotting time determined from the data was correlated to a "gold-standard" clinical measurement of clotting time.

Impedance Measurement Using the AD5933

The AD5933[8] fully integrated single-chip impedance analyzer (Figure 1) is a high-precision impedance-converter system that combines an on-board frequency generator with a 12-bit, 1 MSPS, analog-to-digital converter (ADC). The frequency generator provides an excitation voltage to an external complex impedance at a known frequency. The response signal (current) is sampled by the on-board ADC, and a discrete Fourier transform (DFT) is processed by an on-board DSP engine. The DFT algorithm returns real (R) and imaginary (I) data-words at each output frequency. Using these components, the magnitude and relative phase of the impedance at each frequency point along the sweep can be easily calculated.

The block diagram of the AD5933 demonstrates the full integration of the impedance-measurement system. Local digital processing enables the calculation of the complex impedance of the circuit under test. The system requires initial calibration: a precision resistor is substituted for the impedance to be measured; and a scaling factor is calculated for subsequent measurements. The AD5933 can measure impedance values between 100 Ω and 10 MΩ to a system accuracy of 0.5% for excitation frequencies from 1 kHz to 100 kHz.

The correlation of blood clotting with impedance changes has long been established in the literature.[9,10,11,12,13] However, the recent availability of integrated-circuit complex-impedance measuring devices means that the blood clotting time measurement instrument can be miniaturized. This offers significant advantages in terms of power savings, portability, and final instrument footprint, a key consideration in the critical-care setting.

Single-supply devices, such as the AD5933, often center signal swings around a fixed value of dc bias. This is not an important consideration in most impedance measurements, but dc voltages above a specific threshold cause electrochemical processes to take place in aqueous conducting media in contact with electrodes, altering the sample. To prevent this electrolysis from

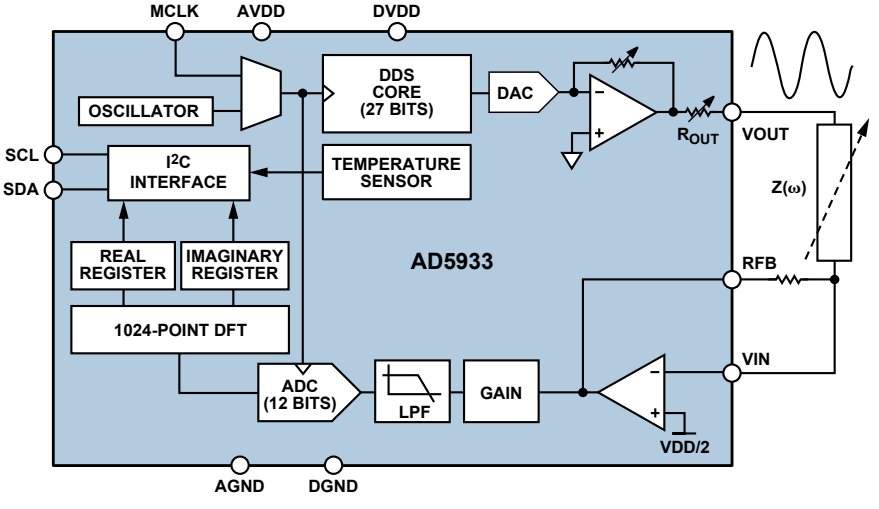

Figure 1. Functional block diagram of impedance-measurement system.

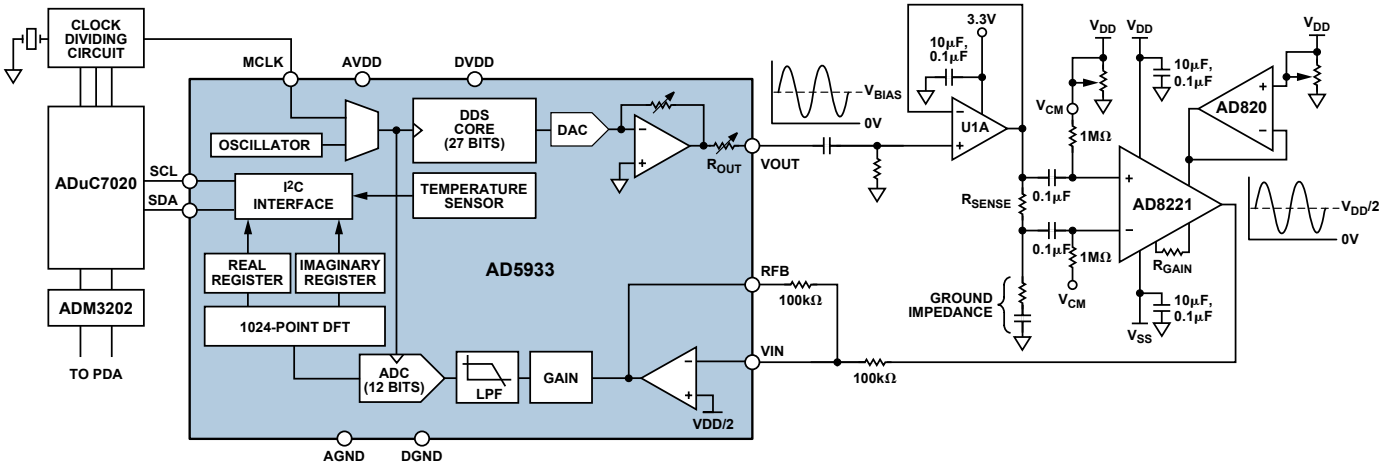

Figure 2. AD5933 with output signal conditioning.

occurring in blood-sample measurements with the AD5933 in the current project, the voltage excitation and the current measurement were ac-coupled using the signal conditioning circuit shown in Figure 2.

The Blood-Coagulation Measurement System

The interface between the blood-sample delivery and the measurement instrumentation is critical. In this case, a specific microfluidic channel into which the blood sample was delivered was designed to connect to the AD5933 instrumentation circuit (Figure 3). The microfluidic device consists of three layers. The bottom layer comprises two screen printed electrodes, which were connected to the input/output port pins of the AD5933 circuit. The top micromolded polymer channel consists of two reservoirs connected via a microchannel. The chemical reagents that modulate the clotting reaction can be contained either within this microchannel or on the central bonding layer. The top- and bottom channels are bonded using a pressure-sensitive adhesive (PSA). The blood sample applied to one reservoir filled the microchannel. This was contacted by the screen-printed electrodes, which were in turn interfaced to the AD5933 circuit.

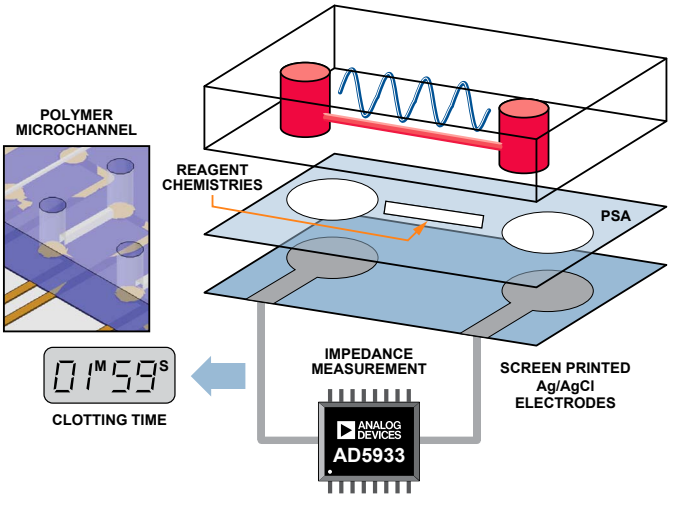

Figure 3. A schematic illustration of the impedance-measurement system with the polymer microchannel that contains the blood sample to be measured. It allows the sample to interact with the specific reagents that modulate the clotting event, and creates the interface between the sample and the AD5933 instrumentation.

Measured Impedance Responses

Impedance response curves of a clotting and nonclotting blood sample are compared in Figure 4. The arrow on the figure indicates the point at which the clotting time of the sample is established.

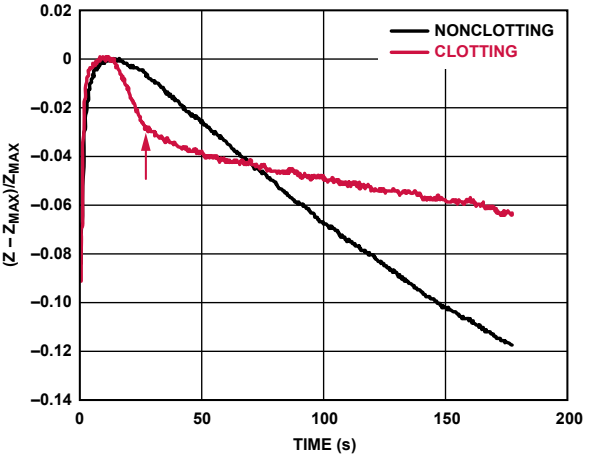

Figure 4. Comparison of impedance profiles for a nonclotting (black) and clotting (red) blood sample.

The impedance response of Figure 5 shows the increase in clotting time with increasing concentrations of heparin in the blood sample. The arrows indicate the clotting time of the different samples.

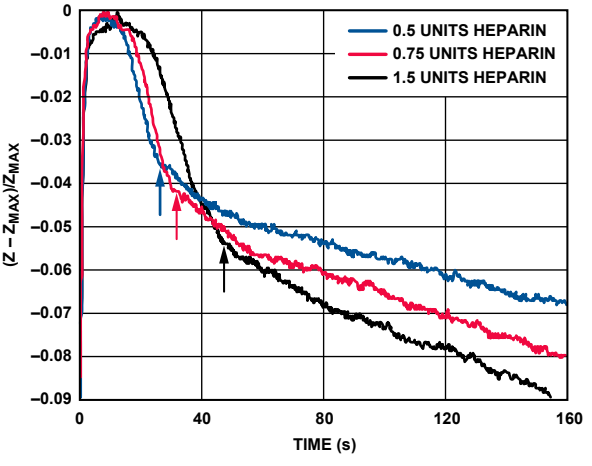

Figure 5. Comparison of impedance profiles for increasing clotting times: shortest (blue) to longest (black).

The clotting times of a number of clinically relevant blood donor samples were measured using the system described above, and these were correlated with measurements performed on the sample donor samples, using the clinical gold-standard measurement system (Figure 6).

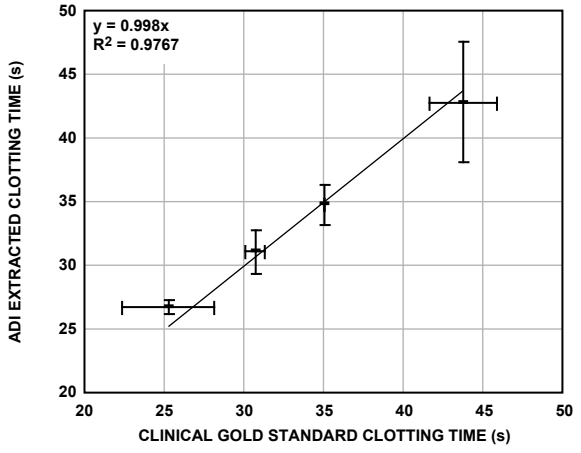

Figure 6. Correlation of extracted clotting time measured using the AD5933 measurement system vs. the clinical gold-standard measurement of clotting time, n = 6 for each sample.

CONCLUSION

The AD5933 single-chip impedance analyzer has been successfully applied to the measurement of blood-impedance changes during coagulation. It offers flexibility, power, and size advantages to the end user over the existing commercially available solutions. Combining integrated-circuit technologies of this sort with new technologies in other media, such as microfluidics and sample handling, provides a powerful platform for future medical device research and development.

ACKNOWLEDGEMENTS

The material in this article is based upon work supported by the Science Foundation Ireland under Grant No. 05/CE3/B754. Thanks to Dermot Kenny, Gerardene Meade, Sarah O'Neill, and all at the Department of Molecular and Cellular Therapeutics at Royal College of Surgeons in Ireland for provision of facilities and expertise. Thanks to Nigel Kent for the microfabrication work—and to the Coagulation Monitor research team at the Biomedical Diagnostics Institute, DCU, Dublin, led by Principal Investigator, Dr. Tony Killard.

REFERENCES

[1] Bowers, John and James J. Ferguson. "Use of the Activated Clotting Time in Anticoagulation Monitoring of Intravascular Procedures." *Texas Heart Institute Journal*. 20 (4). 1993. 258–263.

[2] Kost, Gerald, J., ed. *Principles and Practice of Point-of-Care Testing*. Lippincott Williams & Wilkins. 2002.

[3] www.bdi.ie

[4] www.sfi.ie

[5] www.dcu.ie

[6] Guest, M.M. "Circulatory Effects of Blood Clotting, Fibrinolysis, and Related Hemostatic Processes." *Handbook of Physiology, Circulation III*, American Physiological Society. Washington, DC. 1964.

[7] Brummel-Siedins, K., T. Orfeo, Jenny N. Swords, S.J. Everse, and K.G. Mann. "Blood Coagulation and Fibrinolysis." Chapter 21 in *Wintrobe's Clinical Hematology*. 11th edition. Volume 1. M.M. Wintrobe and J.P. Greer, eds. Lippincott Williams & Wilkins. 2004.

[8] ADI website: www.analog.com (Search) AD5933 (Go)

[9] Ur, A. "Changes in the electrical impedance of blood during coagulation." *Nature* 226. 1970a. 269–270.

[10] Ur, A. "Determination of blood coagulation using impedance measurements." *Biomedical Engineering* 5 (7). 1970b. 342–345.

[11] Ur, A. "Detection of clot retraction through changes of the electrical impedance of blood during coagulation." *American Journal of Clinical Pathology* 56 (6). 1971. 713–717.

[12] Ur, A. "Analysis and interpretation of the impedance blood coagulation curve." *American Journal of Clinical Pathology* 67 (5). 1977. 470–476.

[13] Theiss, W. and A. Ulmer. "Comparative and direct measurement of the electrical impedance in blood coagulation." *Thrombosis Research* 13. 1978. 751–765.

THE AUTHORS

Helen Berney [helen.berney@analog.com], a research engineer with the Healthcare Products Division, joined Analog Devices in February 2006. She is a graduate of Dublin City University with a BSc in Biotechnology, and has a PhD in the area of silicon-based immunosensing diagnostics from University College, Cork, Ireland. Previously, she worked on the development of sensors and integrated systems for biomedical applications at National Microelectronics Research Centre, Cork. She was awarded a Leverhulme Fellowship to work at the Centre for Nanoscale Science and Technology at the University of Newcastle-upon-Tyne, UK, on the development of microelectronics and nanotechnology for biomedical research innovation.

J.J. O'Riordan [jj.oriordan@analog.com], after graduating from the University of Limerick in 1984 with a BEng degree, joined the Test Development department of Analog Devices Limerick (Ireland). In 1998 he received his Master's in Computer Systems—also from the University of Limerick. Specializing in test technology development, he has developed test programs for the first ADI MicroConverter® products and test capability for high-resolution DACs, Σ-Δ converters, low-leakage switches, and other products. More recently, J.J. has been working in healthcare technology, where he designed and built products such as a blood-coagulation monitor and a glucose meter. In his spare time, J.J. enjoys all kinds of sports and is an ICF-certified life and business coach.

Maintaining Public Railways with Lower Cost and Improved Safety

By Anders Norlin Frederiksen and Marco Schmid

A new, systematic maintenance approach now makes it possible to measure, locate, and fix rail- and tramway defects when they appear. Mature railway-engineering know-how and cutting edge technologies—including Blackfin® processors and graphical system design techniques—combine to improve and optimize public transportation.

Over the last decade, public transport by rail or tram has become a popular means of transportation. The number of passengers seeking a comfortable and safe ride is constantly rising. The increased loads call for higher train speeds and shorter stop intervals, thus exposing rails and tramways to increased mechanical stress. This, in turn, causes unavoidable early wear and annoying or dangerous defects (Figure 1).[1] Dealing with the results of these stresses on rails and tramways requires increased emphasis on monitoring and maintenance. Analog Devices Blackfin[2] processors and National Instruments graphically programmable LabVIEW™[3] technology can play a central role in rail inspection systems, acquiring accurate measurements of field data, and storing it for further action. This can result in longer operation lifetimes for rails, improving economy and reliability in the public transport service.

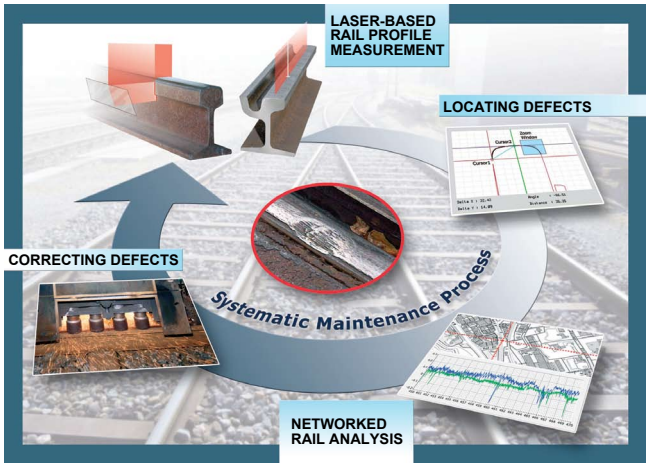

Figure 1. A systematic rail maintenance concept includes measuring, locating, and fixing rail defects.

Rail Tracks—a View "Under the Hood"

When new rail- and tramways are laid out properly, quality assurance verifies correct track positions prior to concreting. Inevitably, as time passes after installation, defects may start to creep in during daily operation. These defects are caused by the stresses of mechanical contact between the wheels and the rails as part of a highly complex spring-mass model, with dynamics ranging from the train's chassis and loading to the railway foundations. In Europe, the critical parameters and tolerance windows of the defects are classified according to railway engineering standards.[4–16] The goal of rail maintenance programs is to discover and measure the irregularities—and keep them at acceptable levels.

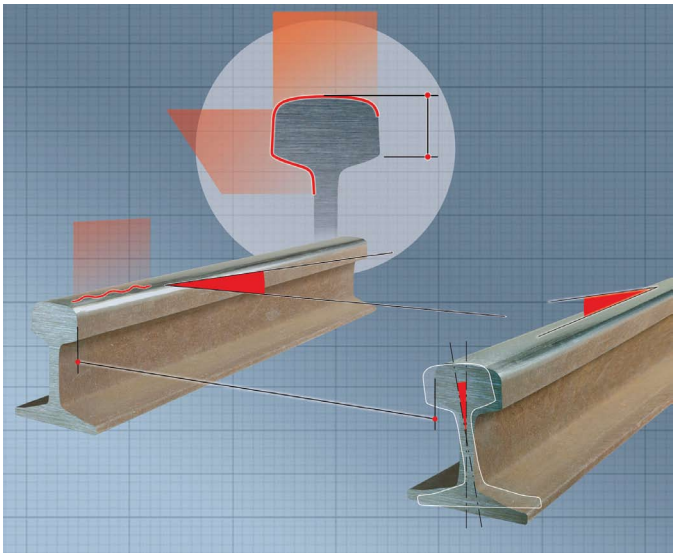

Figure 2. Rail parameters are divided into track geometry, longitudinal profiles, and cross sections.

Rail Track Geometry

The track gauge, or distance between two rails, affects the side-to-side motion of the train. This motion keeps the spot where the wheel and rail meet constantly moving to minimize wear-out.

Variation in the track inclination can make passing trains shake and shudder. Typically caused by yielding of the railway foundations, inclination defects can also be caused by surface irregularities such as corrugations and holes. Some systematic inclination profiles, such as banking, are necessary, however, to minimize passenger discomfort caused by acceleration forces when a train is riding into and out of a curve.

The correct track-to-track spacing prevents any chance of collision when trains are passing one another at high speed.

Longitudinal Surface Profiles

Cracks and breakouts are among the most feared defects, since they can lead to catastrophes such as derailing. Corrugations—wavy irregularities with a characteristic wavelength from 20 mm to 100 mm—are annoyingly noisy when their amplitudes exceed 0.05 mm. With 0.3-mm peaks, on the other hand, the vibration can cause irreversible damage to the railway bed. Corrugations move along the rails, and science is still not clear on where they originate. Single holes are mostly generated by turning or jumping wheels and can be described mathematically with polynomials. They're responsible for the sudden bumps on a tramway ride. Regular bumps that are often experienced on older railways are due to the welding interfaces of the 18-meter railway sections.

Cross Sections

The head geometry of a newly installed rail follows an exactly calculated contact geometry, which optimizes the critical wheel-to-rail interface. The shape is described by tangential lines and specific radii, providing horizontal guidance to allow the wheel to roll off economically, smoothly, and safely (Figure 2).

Measure the Rails

The key requirement for systematic and target-oriented rail maintenance is comprehensive knowledge about the current state of the rail- or tramway network's geometry. This is achieved by a smart measuring strategy that combines odometer results (distance measuring), track geometry, longitudinal profiles, and cross sections with exact GPS locations. All these parameters are acquired by mobile metering devices or well-instrumented measuring vehicles. The measurement data is initiated and preprocessed by Analog Devices Blackfin processors, then finally transferred into high-level analysis software that allows post-analyzing and pinpointing of the measurements and defects on a digital map (Figure 3).

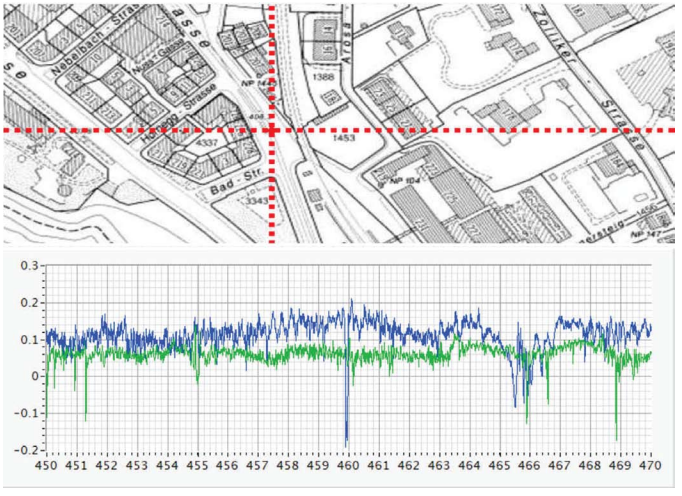

Figure 3. Measurements are combined with GPS data to pinpoint them in *geographic information systems* (GIS).

Track Geometry

The rail gauge is measured using no-contact inductive sensing with accuracies in the 0.01-mm range. Software-based FIR (finite-impulse-response) low-pass filters suppress high-frequency noise, while subsequent moving-average filters ensure that no "pseudo-peaks" occur in a result that is expected to be continuous.

A similar approach is applied to the inclination sensor, which operates like an electronic liquid-level—with an angular range of ±10° and an accuracy to within <0.025°. The physical principle used limits the frequency range to less than 1 Hz.

Measuring the track-to-track distance requires a set of complex and computationally demanding floating-point algorithms to compute the absolute horizontal and vertical distance (Figure 4).

A high-precision laser beam, attached to the side of a vehicle, wobbles ±5° within a distance range of 1 m to 5 m, under the control of a Blackfin processor. The profile of the neighboring rail is low-pass and median filtered, and transformed from polar to Cartesian coordinates. Further processing, such as vector-rotation and resampling, is applied before the profile passes through a pattern matching algorithm. The goal is to find the exact vector to a characteristic geometric feature within the railhead. Because many obstacles, such as rocks or grass, can be found on railways, this vector is passed through a plausibility checker and a tracking algorithm—to ensure reliable and valid results. All this is done in a 5-Hz loop under real-time conditions.

Longitudinal Profiles

High-speed eddy-current sensors record both rail surfaces with micrometer-grade accuracy (Figure 5). A linear encoder processes signals from a magnetic ring that serves as an odometer and a trigger for the analog-to-digital converters. This signal then goes through a FIR band-pass filter, reducing the spectrum to its characteristic wavelengths. Besides the surface profile, metallurgical irregularities, such as partial hardenings and welding points, are recorded.

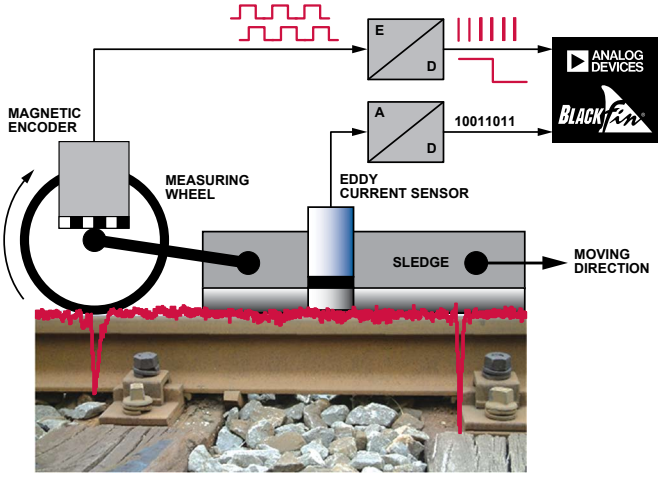

Figure 5. Longitudinal rail profiles are acquired by no-contact eddy-current sensors, pulsed by magnetic encoders.

Cross Profiles

Laser technology is today's state-of-the-art noncontact measuring principle to get the exact cross section of a rail head. Depending on the required accuracy or capturing speed, either traversing laser beams or laser "curtains" (Figure 6) are used to do the job. Raw profiles are linearized, scaled, and spike filtered in real time.

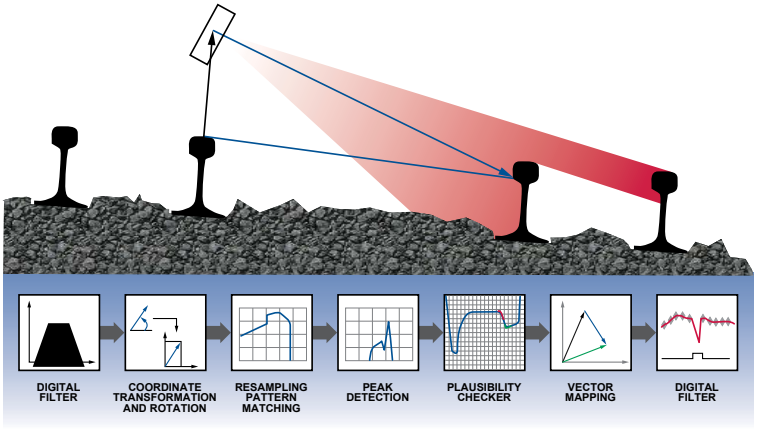

Figure 4. Measuring the track-to-track distance (horizontal and vertical) demands high-performance digital-signal-processing algorithms in real time.

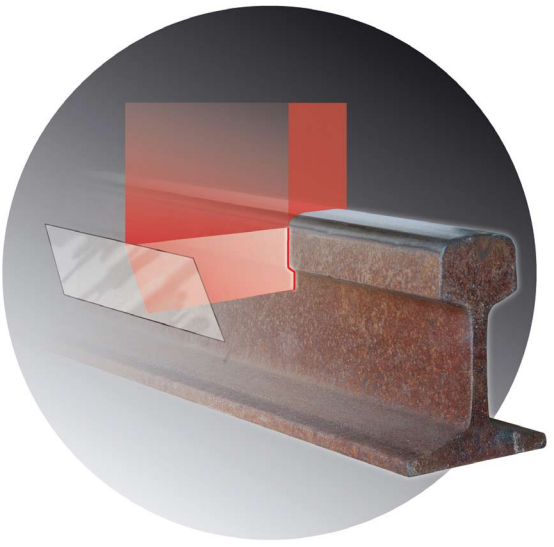

Figure 6. Rail profiles are captured by high-speed laser scanners.

Older Technology—Metering Devices

Until recently, maintenance staffs used many different metering devices to identify cracks and variances on the rails. Each methodology specialized in recording one specific rail defect, but with few exceptions these mechanical methods lacked precise and reproducible results. In recent years, industrial solutions providers, such as Schmid Engineering, embedded advanced processor technology and state-of-the-art components and methodology into their designs. Such advances in the railway infrastructure business gradually led to mobile and multifunctional rail measuring by smart metering devices.

Rail monitor devices (Figure 7) use state-of-the-art technology to simultaneously measure the cross-section profile of the rail, the head height, track gauge, inclination, depth, and ambient temperature—all of which are detected and logged at specifically identifiable locations.

Figure 7. Rugged environments and tight schedules demand light, easy-to-use, and productive metering devices.

All key characteristics are processed and visualized on site and stored to removable memory. The RailSurf sled (Figure 8) continuously monitors and records longitudinal track parameters, as an operator or a vehicle pulls it along the rails. It carries several sensors, mapping problems such as corrugations, holes, cracks, and variations in rail gauge and inclination. The resulting information can be stored in removable memory or wirelessly transmitted to an operator interface.

Figure 8. The RailSurf sled, driven by Blackfin processors and LabVIEW embedded modules, records longitudinal wavy irregularities. A GPS receiver and inclination sensor are built into the operator panel.

Blackfin Processor as the Heart of the System

The Blackfin processor, as the *heart* of these portable test tools, empowers the convergence of microcontroller and DSP technology by offering dynamic power management for economical battery operation. The MCU circuitry conveniently interfaces with scalable input/output (I/O), such as laser scanners, analog and digital sensors, keyboards, TFT (thin-film-transistor) displays, battery/fuel gauges, and removable media. The DSP portion is dedicated to advanced digital algorithms, such as filters, transforms (FFTs, for example), determination of geometric residuals, or other demanding computational tasks. Recent advancements in graphical system design by LabVIEW embedded modules, with their high-level block diagrams and dataflow-oriented language, offer a direct programming model of the Blackfin processor. This high-level approach with ready-to-use mathematical-analysis blocks and graphical multitasking moves functionality to the next higher level of digital embedded design.

Measuring Machines

A multifunctional vehicle that is driven by a set of five interlinked Blackfin processors is able to record rail parameters for up to 10 km of a railway section with 5-mm point-to-point resolution.

Blackfin Processor #1 allows user interaction over a keyboard and two TFT displays. Processor #2 records track geometry and longitudinal profiles at high speed and embeds GPS information into the measurements, which are then received by Processor #3. Together with cross sections that are captured by Processor #4, all the data is finally streamed to Processor #5, which stores the huge amount of data in large RAM buffers to be eventually saved to binary files on removable media.

Locate the Defects

The acquired measurements are fed into a common software platform that links track geometry, longitudinal profiles, and cross sections with GPS locations and odometer information. Realized with LabVIEW and its toolkits, this platform serves as a common data-exchange and -analysis tool. It interfaces to a variety of measurement devices, vehicles, and maintenances machines. Smart filters applied to the measurements function like an X-ray to locate critical rail defects. The result is a true digital representation of the whole rail geometry. This essential information is then directly usable for actions such as rail repair or exchange. The final data log is wirelessly connected to external databases and CAD software to transfer the results into any customer's IT environment.

Smart, Powerful LabVIEW Filters Find Defects

Smart LabVIEW filters sift through longitudinal data to find symptoms of interest. Corrugations get detected through a fast-Fourier-transform (FFT) analysis, watching for the characteristic wavelengths in the longitudinal profile. Holes are tracked by comparing the measured profile with memorized patterns and the simulation of the mechanical rail-wheel contact. Cracks show significant transients, so they can be detected by differentiating a moving data window. Finally, unique vibration patterns in the inclination profile are located by continuously running and evaluating analytical models.

The resulting symptoms are also fed into correlating "super-algorithms." Here the information is either reduced even more, or additional high-level information is extracted from the measured data. An *inclination* indication, for example, is interpreted as meaningless and is rejected if it is not accompanied by a related signal peak on the rail surface. On the other hand, a cross profile indicating significant wear-out or a longitudinal crack will trigger an alarm.

The main technique used in the evaluation of rail cross sections is comparing a measured profile with a reference. Algorithms based on vector mathematics and stochastic methods align and overlay the two profiles to allow computation of critical characteristics. Vertical and perpendicular residuals directly indicate wear-outs (Figure 9).

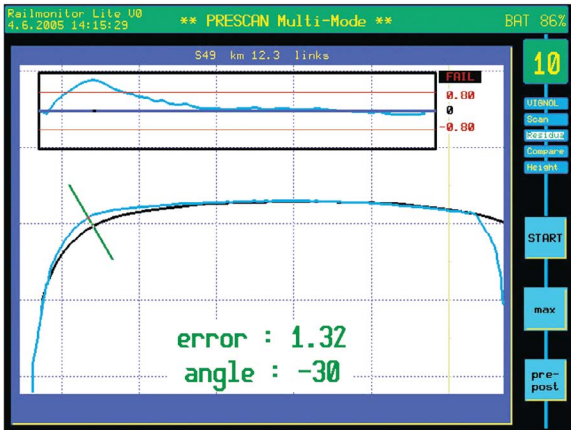

Figure 9. Smart cross-profile analysis algorithms take advantage of the Blackfin processor's speed and capacity to indicate irregularities in real time and on site.

Other parameters include the remaining head height, a correct and well-shaped rail radius (Figure 10), or the gap of an active, closed track switch. Keeping within switch tolerances is a key requirement to avoid the danger of derailing high-speed trains passing the switches. Rail operating companies focus on thorough monitoring of the switches.

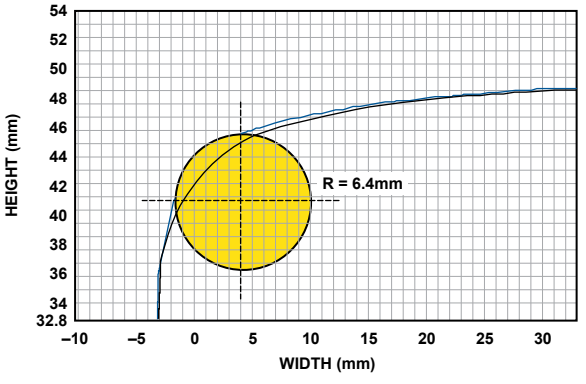

Figure 10. Determining the rail radius calls for complex mathematical functions.

Rail engineers can adjust filter-parameter tolerance windows to separate "pseudo-warnings" from true rail defects that significantly influence passenger comfort and transportation safety.

Pinpointing Defects on a Digital Map

GPS information that is embedded in the data allows the located defects to be pinpointed on a digital map. This geographical information adds significant knowledge and new context about locations of railway *hot-spots*, such as tight curves, switches, and stations. This "Easy-GIS" geographic information system has been made available with the image-processing features of LabVIEW. An existing bitmap of the region of interest, for example, a city, is broken down into single tiles, each given the exact map coordinates. As the rail engineer browses through the set of defects, LabVIEW continuously loads the corresponding tiles from the hard drive into memory and assembles them to form a single JPEG image. This image is then copied into a LabVIEW plot-chart indicator and overlaid with a digital cursor at exact locations of the defects.

Distribute Results to Other Applications

The results are finally transferred to and from higher-level applications. Geometric profiles of critical defects, such as wear-outs and holes, can be exchanged with standard CAD systems for further analysis. This is achieved by the *Drawing-eXchange* (file) *Format* (DXF).

Connection to external database management systems is established through *ActiveX Data Objects* (ADO), which use Universal Data Links (UDL) for the connection type and path. A set of high-level virtual instruments (VIs) allows the data platform to perform the most common database tasks such as addressing tables and exchanging data.

The VAG Nuremberg Transport Corporation maintains a matrix of predefined and critical locations in a Microsoft Access database, which is continuously screened for variations. As soon as some hot-spots exceed a tolerance window, an electronic maintenance plan is created and deployed to the measuring devices in the maintenance machines.

The maintenance concept at Zurich Public Transport (*Verkehrsbetriebe Zürich, VBZ*) relies on a commercial GIS tool with a built-in MS Access database. All infrastructure elements—including rail sections, stations, switches, etc.—are listed and can be visualized on a geographical map that represents the whole tram network of the city—at the push of a button. As with Nuremberg, the state of the rails is continuously monitored as a vital part of a short- and long-term maintenance concept. The LabVIEW platform connects to this GIS tool by the means of ActiveX and .NET mechanisms.

Solving the Problem

The resulting maintenance plan fed back from the IT environment is downloaded into the maintenance machines as quality set points. A pair of Blackfin processors supports the team in fixing worn-out or defective rail sections rapidly and systematically, using several iterative grinding runs to bring the rail back into its original shape.

One of the processors provides the operating personnel with a multifunctional keyboard, a visual of the rails on two TFT monitors, and removable memory. Two laser scanners continuously capture snapshots of cross profiles at 20 Hz and transfer the data online to the CPU over a CAN (controller area network). The processor then calculates the deviation from a reference profile and forwards new set points to the underlying grind unit, which is controlled by the other Blackfin processor.

This grind unit consists of a total of six independent grinding pots. Each offers three degrees of freedom with actuators based on a hydrostatic principle. At first the pot moves horizontally either to the inside, outside, or middle of the rail head. Then it rotates to the worst-case deviation and finally moves down until it touches the railhead to start removing the material. The Blackfin processor controls each of these 18 movements simultaneously by applying pulse-width modulated (PWM) signals to the valves that control the hydrostatic actuators. Additionally, six rotation sensors, six translation gauges, 18 no-contact position switches, and six pressure sensors are continuously monitored during this positioning process. While this process took minutes using a traditional approach, the grinding pots are now placed automatically within seconds.

Finally, the grinding pot starts to remove the excess material (Figure 11). Secure and sturdy housings protect the electronics and the sensors from flying sparks, aggressive dust, humidity, and heat.

Figure 11. Electronic maintenance plans are deployed to maintenance machines, which solve the problem on-rail by grinding.

After the grinding process, the quality is assured by loading a set of profile measurements back into the IT environment using removable media.

CONCLUSION

A systematic maintenance concept for rail- and tramways has been taken to the next phase using digital embedded design. By taking advantage of low-level measurement and control on the rails, and high-level data-mining and analysis at a central location, an optimal and cost-effective integrated solution for track maintenance has been designed.

Taking advantage of the scalable performance and capability of a Blackfin processor, the metering devices and vehicles used for measuring/maintenance in this concept have attained the critical real-time behavior and robustness required by the inherent harsh environments.

Locating the defects, as required for high-level data analysis and visualization for this design, has been achieved within the LabVIEW environment—not only to develop the complex mathematical filter algorithms, but also to meet the different connectivity challenges involved in networking the field devices with the IT environments. The ease of use of LabVIEW has once again empowered a high-profile design with optimal possibility for reuse and restructure.

LabVIEW Embedded technology, especially when specialized for Blackfin processors, now opens the doors to a paradigm shift of algorithms normally designed in ASM or C/C++. With the changing technology it is now possible, in cases like this, to optimize the process of locating defects (principally cracks) in any rail or tram system. All data on any defects is stored in centralized databases for either an immediate fix or monitoring. The RailSurf measuring sled is the first example of a mobile and smart metering device, which brings to life this next generation of embedded solutions, embodying a maintenance concept that is fast, environmentally sound, and cost-effective.

REFERENCES

[1] "Vernetzte Schienenmess- und Schleiftechnik." *EI-Der Eisenbahningenieur*. Ausgabe 6/2007.

[2] www.analog.com/blackfin.

[3] www.analog.com/en/embedded-processing-dsp/blackfin/labview_emb_bf/processors/product.html.

[4] *Bahnanwendungen—Oberbau—Abnahme von Arbeiten*. EN13231-3 ÖNORM.

[5] *Katalog der wichtigsten Schienenfehler in Gleisen und Weichen*. Richtlinie 821.2017.Z01DB.

[6] *Prüfung der Gleisgeometrie mit Gleismessfahrzeugen*. Richtlinie 821.2001.

[7] *Prüfung des Schienenkopflängsprofils*. Richtlinie 821.2008.

[8] *Stosslückenprüfung*. Richtlinie 821.2009.

[9] *Zulässige Abnutzung der Schienen im Gleis*. Richtlinie 821.2011.

[10] *Langwellige Gleislagefehler messen und erkennen*. Richtlinie 824.0520.

[11] *Messeinrichtungen und Handmessgeräte*. Richtlinie 824.0540.

[12] *Bearbeitung von Weichen*. Richtlinie 824.4016.

[13] *Schienenbearbeitung in Gleisen*. Richtlinie 824.4015.

[14] *Neuschienen bearbeiten*. Richtlinie 824.4010.

[15] *Schienenbearbeitung planen*. Richtlinie 824.4005.

[16] *Schienenbearbeiten Grundlagen*. Richtlinie 824.4001.

THE AUTHORS

Anders Norlin Frederiksen

[anders.frederiksen@analog.com] received his BScEE (honors) from the Technical University of Denmark in 1994 and served as an assistant professor at the Technical University of Denmark (1995–97). He joined Analog Devices in 1998 as a systems engineer on power electronics and control in Norwood, Massachusetts. Since then he has had various roles within the organization; currently he is a Worldwide Industrial Marketing Manager.

Marco Schmid [marco@schmid-engineering.ch] is a senior engineer at Schmid Engineering, Switzerland. After gaining his Master of Engineering Technology degree in systems science in 1993, he was engaged in hardware and software development for DSP products. Since 1997, as head of an internationally active embedded-system-solution provider, he focuses on systems integration and high-level graphical system design on microprocessors.

ANALOG ICs POWER DIGITAL TVs *(continued from Page 2)*

CW, FOX, ION, NBC, PBS, and independent stations, they will be able to receive free high-definition broadcasts on their HD television sets or standard-definition pictures on their converter-box-equipped analog TVs. *Multicasting* will increase the number of digital programs that can be received. In Boston's suburbs, for example, more than 40 channels are available with a modest antenna and an HDTV or converter box.[i]

Although analog TV broadcasts are ending and analog TV sets are no longer being manufactured, analog *circuitry* is far from dead. Contrary to popular belief, more analog content is found in a modern "digital" high-definition TV than in older analog TV sets. As the figure shows,[ii] Analog Devices makes a variety of video amplifiers, decoders, encoders, and filters to convert legacy analog RGB, composite video, S-Video, and component video signals from analog to digital and back again. HDMI™ buffers, multiplexers, receivers, and transmitters support the use of long cables, allowing multiple components, such as *audio-video receivers* (AVR), Blu-ray Disc® players, and video games to be interconnected with the TV. Display drivers provide the high-voltage drive signals, control clocks, gamma correction, and other circuitry required to interface with the LCD display panel. RF splitters enable the use of multiple tuners for picture-in-picture and digital video recorder (DVR) functions. Audio processors and Class-D amplifiers provide multichannel surround sound; and audio amplifiers, ADCs, and DACs provide support for legacy system components. Up to 20 power supplies can be found in a state-of-the-art LCD HDTV, so low-dropout regulators and analog power management, monitoring, and sequencing devices are required. In addition, Analog Devices Blackfin® and SHARC® digital signal processors handle much of the real-time signal processing and control in today's HDTVs.

Advanced television systems demand the highest-performance signal processing solutions in an extremely cost-sensitive market. From RF to baseband video to audio to power management, building on a framework of industry-leading core technologies, Analog Devices Advantiv® advanced television solutions enable lifelike audio and video, offering the widest range of analog, digital, and mixed-signal solutions to solve the most difficult multiformat advanced television challenges.[iii]

[i] Antenna Web
www.antennaweb.org/aw/welcome.aspx

[ii] Advanced Television Signal Chain
www.analog.com/en/video--imaging-solutions/advanced-television/applications/index.html

[iii] Advantiv Advanced Television Solutions
www.analog.com/static/imported-files/overviews/898928192AdvancedTV_BrochureFinal.pdf

Scott Wayne [scott.wayne@analog.com]

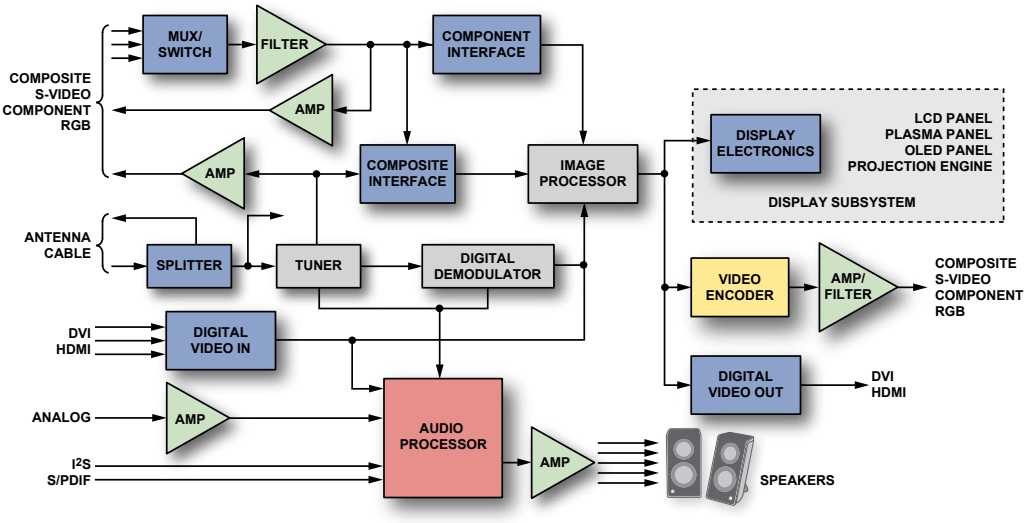

PRODUCT INTRODUCTIONS: VOLUME 42, NUMBER 3

Data sheets for all ADI products can be found by entering the model number in the search box at www.analog.com.

July

ADC, SAR, 8-channel, 14-bit, 250-kSPS **AD7949**
ADCs, SAR, 4-/8-channel, 16-bit, 250-kSPS **AD768x**
Amplifier, RF Driver, 2.3-GHz to 4.0-GHz **ADL5321**
Driver, Pin, dual, 4-Gbps data rates **ADATE209**
Multiplexer/Demultiplexer, quad 2:1, 6.5-Gbps **AD8158**
Sensors, Temperature, trip-point switch **ADT640x**
Transceivers, RS-485, isolated **ADM248xE**

August

ADC, SAR, dual, 12-bit, 1-MSPS **AD7262**
Amplifier, IF, dual, 20-MHz to 500-MHz **ADL5534**
Amplifier, Variable-Gain, RF, 250-MHz to 2400-MHz **ADL5592**
Modulator, Sigma-Delta, isolated **AD7401A**
Multiplexer, *i*CMOS, 4:1, 1.5-Ω **ADG1404**
Switch, CMOS, dual SPDT, 0.8-Ω **ADG854**
Switch, Crosspoint, 8 × 8, asynchronous, 4.25-Gbps **ADN4600**
Switch, *i*CMOS, dual SPDT, 1.5-Ω **ADG1436**

September

Accelerometer, Configurable, *i*MEMS, high-*g* **ADXL180**
ADCs, SAR, 6-channel, 16-/14-/12-bit, 250-kSPS **AD765x-1**
Amplifier, Audio, 3-W, Class-D **SSM2319**
Amplifier, Instrumentation, 1-ppm/°C gain drift **AD8228**
Amplifier, Instrumentation, 20-nV/°C offset drift **AD8293**
Amplifier, Operational, dual, micropower **ADA4505-2**
Amplifier, Operational, quad, micropower **AD8508**
Buffer, HDMI/DVI, with equalization **AD8195**
Codec, Audio, low-power **SSM2604**
Converter, Resolver-to-Digital, 10-bit to 16-bit **AD2S1210**
DACs, Voltage-Output, quad, 12-/14-/16-bit **AD50x4**
DACs, Voltage-Output, quad, 12-/14-/16-bit **AD57x4**
Driver, Backlight, with I/O expander **AD5520**
Driver, Half-Bridge, isolated **ADuM6132**
Driver, Laser-Diode, 50-Mbps to 4.25-Gbps **ADN2873**
Driver/Receiver, RS-232, isolated **ADM3251E**
Front-End, Analog, 900-MHz ISM-band **ADF9010**
Front-End, Mixed-Signal, WiMAX **AD9352-5**
Front-Ends, Mixed-Signal, WiMAX/WiBro **AD935x**
Multiplexer, *i*CMOS, 8-channel differential **ADG1407**
Multiplexer, *i*CMOS, 16-channel single-ended **ADG1406**
PMU, 250-MHz, includes DCL **ADATE305**
PMU, 500-MHz, includes DCL **ADATE302-02**
PMU, Quad, 16-bit level-setting DACs **AD5522**
Regulator, Low-Dropout, 150-mA loads **ADP121**
Regulator, Low-Dropout, 350-mA loads **ADP130**

Analog Devices, Inc.
Worldwide Headquarters
Analog Devices, Inc.
One Technology Way
P.O. Box 9106
Norwood, MA
02062-9106 U.S.A.
Tel: 781.329.4700
(800.262.5643,
U.S.A. only)
Fax: 781.461.3113

Analog Devices, Inc.
Europe Headquarters
Analog Devices, Inc.
Wilhelm-Wagenfeld-Str. 6
80807 Munich
Germany
Tel: 49.89.76903.0
Fax: 49.89.76903.157

Analog Devices, Inc.
Japan Headquarters
Analog Devices, KK
New Pier Takeshiba
South Tower Building
1-16-1 Kaigan, Minato-ku,
Tokyo, 105-6891
Japan
Tel: 813.5402.8200
Fax: 813.5402.1064

Analog Devices, Inc.
Southeast Asia
Headquarters
Analog Devices
22/F One Corporate Avenue
222 Hu Bin Road
Shanghai, 200021
China
Tel: 86.21.2320.8000
Fax: 86.21.2320.8222

Purchase of licensed I²C components of Analog Devices or one of its sublicensed Associated Companies conveys a license for the purchaser under the Philips I²C Patent Rights to use these components in an I²C system, provided that the system conforms to the I²C Standard Specification as defined by Philips.

©2008 Analog Devices, Inc. All rights reserved. Trademarks and registered trademarks are the property of their respective owners.
Printed in the U.S.A. M02000423-39-10/08

ANALOG DEVICES